J|A|C|S
ARTICLES
Published on Web 05/12/2006

Conformational Stabilization of an Engineered Binding Protein

Elisabet Wahlberg† and Torleif Härd*,‡

Contribution from the School of Biotechnology, Royal Institute of Technology (KTH), S-106 91 Stockholm, Sweden, and Department of Medical Biochemistry, Göteborg University, Box 440, S-405 30 Göteborg, Sweden

Received February 8, 2006; E-mail: torleif.hard@medkem.gu.se

Abstract: We analyzed the thermodynamic basis for improvement of a binding protein by disulfide engineering. The Z_{SPA-1} affibody binds to its Z domain binding partner with a dissociation constant K_d = 1.6 μM, and previous analyses suggested that the moderate affinity is due to the conformational heterogeneity of free Z_{SPA-1} rather than to a suboptimal binding interface. Studies of five stabilized Z_{SPA-1} double cystein mutants show that it is possible to improve the affinity by an order of magnitude to K_d = 130 nM, which is close to the range (20 to 70 nM) observed with natural Z domain binders, without altering the protein−protein interface obtained by phage display. Analysis of the binding thermodynamics reveals a balance between conformational entropy and desolvation entropy: the expected and favorable reduction of conformational entropy in the best-binding Z_{SPA-1} mutant is completely compensated by an unfavorable loss of desolvation entropy. This is consistent with a restriction of possible conformations in the disulfide-containing mutant and a reduction of average water-exposed nonpolar surface area in the free state, resulting in a smaller conformational entropy penalty, but also a smaller change in surface area, for binding of mutant compared to wild-type Z_{SPA-1}. Instead, higher Z domain binding affinity in a group of eight Z_{SPA-1} variants correlates with more favorable binding enthalpy and enthalpy−entropy compensation. These results suggest that protein−protein binding affinity can be improved by stabilizing conformations in which enthalpic effects can be fully explored.

Introduction

In protein engineering it is common to introduce cysteine residues that can oxidize to form stabilizing disulfide bonds. A number of studies demonstrate that proper disulfide engineering can dramatically increase the thermal and chemical stability of folded proteins,[1−3] improve protein function,[4,5] or be used to lock a protein into a desired conformation.[6] Classical theory predicts that disulfide bonds stabilize proteins by reducing the conformational entropy of the unfolded state,[7−9] but experimental studies show that significant changes in stabilizing folding enthalpy also occur.[10−12] The effect of disulfides on protein stability can therefore be both entropic and enthalpic. Disulfide engineering has also, in a few cases, been used to improve the properties of engineered binding proteins.[13,14] However, the thermodynamic basis for improving binding affinity by conformational stabilization has not previously been investigated.

We use a class of engineered binding proteins called affibody proteins to study structure and thermodynamics of molecular recognition in protein−protein complexes.[15−19] Affibody proteins are based on the 58-residue three-helix Z domain.[20] Affibody binders are selected by a phage display of Z domain libraries in which 13 residues on the surface of helices I and II have been subjected to random mutagenesis.[21] Protein ligands to a number of different target proteins have been identified in this way (see for example refs 22−25), and their affinities are

† Royal Institute of Technology (KTH).
‡ Göteborg University.

(1) Matsumura, M.; Signor, G.; Matthews, B. W. *Nature* **1989**, *342*, 291−293.
(2) Mansfeld, J.; Vriend, G.; Dijkstra, B. W.; Veltman, O. R.; van den Burg, B.; Venema, G.; Ulbrich-Hofmann, R.; Eijsink, V. G. H. *J. Biol. Chem.* **1997**, *272*, 11152−11156.
(3) Mårtensson, L. G.; Karlsson, M.; Carlsson, U. *Biochemistry* **2002**, *41*, 15867−15875.
(4) Way, J. C.; Lauder, S.; Brunkhorst, B.; Kong, S.-M.; Qi, A.; Webster, G.; Campbell, I.; McKenzie, S.; Lan, Y.; Marelli, B.; Nguyen, L. A.; Degon, S.; Lo, K.-M.; Gillies, S. D. *Protein Eng., Des. Sel.* **2005**, *18*, 111−118.
(5) Eijsink, V. G. H.; Bjork, A.; Gåseidnes, S.; Sirevåg, R.; Synstad, B.; van den Burg, B.; Vriend, G. *J. Biotechnol.* **2004**, *113*, 105−120.
(6) Shimaoka, M.; Lu, C.; Salas, A.; Xiao, T.; Takagi, J.; Springer, T. A. *Proc. Natl. Acad. Sci. U.S.A.* **2002**, *90*, 16737−16741.
(7) Schellman, J. A. *C. R. Trav. Lab. Carlsberg, Ser. Chim.* **1955**, *29*, 230−259.
(8) Flory, P. J. *J. Am. Chem. Soc.* **1956**, *78*, 5222−5235.
(9) Pace, C. N.; Grimsley, G. R.; Thomson, J. A.; Barnett, B. J. *J. Biol. Chem.* **1988**, *263*, 11820−11825.
(10) Kuroki, R.; Inaka, K.; Taniyama, Y.; Kidokoro, S.; Matsushima, M.; Kikuchi, M.; Yutani, K. *Biochemistry* **1992**, *31*, 8323−8328.
(11) Betz, S. F. *Protein Sci.* **1993**, *2*, 1551−1558.
(12) Vaz, D. C.; Rodrigues, J. R.; Seabald, W.; Dobson, C. M.; Brito, R. M. M. *Protein Sci.* **2006**, *15*, 33−44.
(13) Reiter, Y.; Brinkmann, U.; Lee, B.; Pastan, I. *Nat. Biotechnol.* **1996**, *14*, 1239−1245.
(14) Starovasnik, M. A.; Braisted, A. C.; Wells, J. A. *Proc. Natl. Acad. Sci. U.S.A.* **1997**, *94*, 10080−10085.
(15) Wahlberg, E.; Lendel, C.; Helgstrand, M.; Allard, P.; Dincbas-Renqvist, V.; Hedqvist, A.; Berglund, H.; Nygren, P.-Å.; Härd, T. *Proc. Natl. Acad. Sci. U.S.A.* **2003**, *100*, 3185−3190.
(16) Lendel, C.; Dincbas-Renqvist, V.; Flores, A.; Wahlberg, E.; Dogan, J.; Nygren, P.-Å.; Härd, T. *Protein Sci.* **2004**, *13*, 2078−2088.
(17) Dincbas-Renqvist, V.; Lendel, C.; Dogan, J.; Wahlberg, E.; Härd, T. *J. Am. Chem. Soc.* **2004**, *126*, 11220−11230.
(18) Lendel, C.; Dogan, J.; Härd, T. *J. Mol. Biol.*, accepted (doi:10.1016/j.jmb.2006.04.043).
(19) Dogan, J.; Lendel, C.; Härd, T. *J. Mol. Biol.*, accepted (doi:10.1016/j.jmb.2006.04.041).
(20) Nilsson, B.; Moks, T.; Jansson, B.; Abrahmsén, L.; Elmblad, A.; Holmgren, E.; Henrichson, C.; Jones, T. A.; Uhlén, M. *Protein Eng.* **1987**, *1*, 107−113.

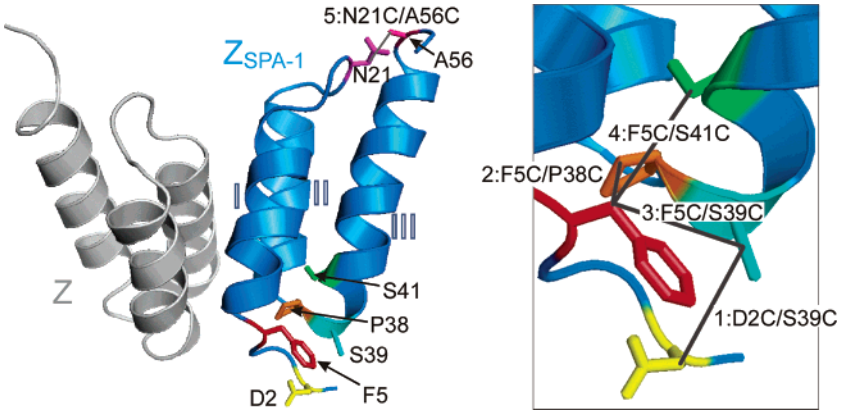

Figure 1. The structure of the Z:Z_{SPA-1} complex showing side chains subjected to cystein mutations in Z_{SPA-1} (left) and a detailed view of sites for mutation in helices I and III (right). The peptide backbones of the Z domain (gray) and Z_{SPA-1} (cyan) are illustrated as secondary structure cartoons, and the three helices have been indicated for Z_{SPA-1}. The locations of disulfides have been labeled according to the notation of mutants used in the text.

in many cases impressive with dissociation constants in the nanomolar range.

The Z_{SPA-1} affibody was selected as a binder to staphylococcal protein A, and it binds to the Z domain, which is derived from this protein.[23] The conformation of Z_{SPA-1} in the free state is molten globule (MG) like[26−29] with reduced secondary structure content, aggregation propensity, and poor thermal stability, and it binds the hydrophobic dye ANS.[15] The average topology of the original Z domain is retained in the MG state, but it is represented by a multitude of rapidly interconverting conformations in which helices I and II are being transiently unfolded.[16] The MG state is therefore also only marginally stable, and a significant fraction of Z_{SPA-1} exists in a completely unfolded state at room temperature. The Z:Z_{SPA-1} complex is formed with a dissociation constant $K_d \approx 1\ \mu$M, whereas binding of the Z domain to the Fc fragment of IgG immunoglobulin occurs with a K_d value of 20 to 70 nM.[30,31] Still, the interaction interface in the Z:Z_{SPA-1} complex is large (ca. 1600 Å^2) and shows tight steric and polar/nonpolar complementarity.[15] A thermodynamic characterization of Z:Z_{SPA-1} binding suggested that forcing the MG state into the ordered three-helix bundle observed in the complex is associated with a conformational entropy penalty.[17] We concluded that it is this conformational transition, rather than the MG-state unfolding equilibrium or any serious deficiency of the binding interface, which is the primary reason for the moderate binding affinity.

We set out to investigate to which extent conformational entropy effects can be reduced and to study the thermodynamic basis for improving protein−protein binding by disulfide engineering. We produced five double-cystein mutants of Z_{SPA-1} in which disulfides might stabilize the affibody in its bound-state conformation without altering the Z domain binding surface (Figure 1). Thermal stability and helical content were analyzed using circular dichroism (CD), and structural homogeneity was assessed from the NMR spectrum. Z domain binding affinities of oxidized and reduced Z_{SPA-1} mutants were measured using isothermal titration calorimetry (ITC), and a full thermodynamic characterization of the best binder was performed. We find that binding affinity can be improved by at least a factor of 10 by conformational stabilization. The effects on binding entropy are two-fold: the unfavorable conformational entropy change on binding is reduced, as expected, but this is counteracted by a loss of favorable desolvation entropy. Instead, the binding affinity of all Z_{SPA-1} variants scales with the binding enthalpy. We explain these observations in terms of the effect of disulfides on the capability of forming a fully binding competent conformation.

Methods

Disulfide Engineering. The NMR structure of Z_{SPA-1} in complex with the Z domain (ref 15; database entry 1h0t.pdb) was inspected to select pairs of amino acid residues suitable for cysteine substitution. Residues involved in binding to the Z domain were conserved in order to preserve the binding interface. First, we considered residue pairs for which a disulfide would link the N-terminal end of helix I to the C-terminal end of helix II without distorting the backbone conformation and modeled these using the Swiss PDB Viewer 3.7 software (www.expasy.org/spdbv/). The χ^1 torsion angles of cystein-substituted side chains were adjusted to allow for S−S bonds with right- or left-handed conformations. The structures were subjected to 500 steps of steepest decent energy minimization and evaluated with respect to total energy, backbone modifications, and the disulfide torsion angle energy.[32,33] The substitutions in mutants 1:D2C/S39C, 2:F5C/P38C, and 3:F5C/S39C were selected in this way. Second, we considered other pairs of side chains that are separated by at least 20 residues in the sequence and for which $C^\gamma-C^\gamma$ and $C^\alpha-C^\alpha$ distances are less than 6 Å (ref 34) and 8 Å, respectively, in the 10 lowest energy structures of the Z:Z_{SPA-1} complex. This resulted in the selection of 4:F5C/S41C, 5:N21C/A56C, and 6:A12C/S41C for which these criteria are fulfilled and good disulfide stereochemistry was judged to be feasible (Figure 1).

(21) Nord, K.; Gunneriusson, E.; Ringdahl, J.; Ståhl, S.; Uhlén, M.; Nygren, P.-Å. *Nat. Biotechnol.* **1997**, *15*, 772−777.
(22) Nord, K.; Nord, O.; Uhlén, M.; Kelley, B.; Ljungqvist, C.; Nygren, P.-Å. *Eur. J. Biochem.* **2001**, *268*, 4269−4277.
(23) Eklund, M.; Axelsson, L.; Uhlén, M.; Nygren, P.-Å. *Proteins: Struct., Funct., Genet.* **2002**, *48*, 454−462.
(24) Sandström, K.; Xu, Z.; Forsberg, G.; Nygren, P.-Å. *Protein Eng.* **2003**, *16*, 691−697.
(25) Wikman, M.; Steffen, A.-C.; Gunneriusson, E.; Tolmachev, V.; Adams, G. P.; Carlsson, J.; Ståhl, S. *Protein Eng. Des. Sel.* **2004**, *17*, 455−462.
(26) Regan, L. *Proc. Natl. Acad. Sci. U.S.A.* **2003**, *100*, 3553−3554.
(27) Semisotnov, G.; Rodionova, N.; Razgulyaev, O.; Uversky, V.; Gripas, A.; Gilmanshin, R. *Biopolymers* **1991**, *31*, 119−128.
(28) Ptitsyn, O. *Trends Biochem. Sci.* **1995**, *20*, 376−379.
(29) Dobson, C. *Current Biology* **1994**, *4*, 636−640.
(30) Jendeberg, L.; Persson, B.; Andersson, R.; Karlsson, R.; Nilsson, B. *J. Mol. Recognit.* **1995**, *8*, 270−278.
(31) Cedergren, L.; Andersson, R.; Jansson, B.; Uhlén, M.; Nilsson, B. *Protein Eng.* **1993**, *6* (4), 441−448.
(32) Weiner, S. J.; Kollman, P. A.; Case, D. A.; Singh, U. C.; Ghio, C.; Alagona, G.; Profeta, S., Jr.; Weiner, P. *J. Am. Chem. Soc.* **1984**, *106*, 765−784.
(33) Katz, B. A.; Kossiakoff, A. *J. Biol. Chem.* **1986**, *261*, 15480−15485.
(34) Matsumura, M.; Becktel, W. J.; Levitt, M.; Matthews, B. W. *Proc. Natl. Acad. Sci. U.S.A.* **1989**, *86*, 6562−6566.

Protein Production. Amino acid substitutions were introduced using the QuikChange site-directed mutagenesis kit (Stratagene) according to the supplier's recommendations, except for the mutations D2C and S39C, where polymerase chain reaction (PCR) with mutagenesis primers was used due to AT-rich sequences in these regions of the DNA. AccuPrime Pfx DNA polymerase (Invitrogen) was used for PCR. The product was digested with NcoI/EcoRI and inserted into the pT7 plasmid, which is a modified pET28a (+) expression vector adding only an N-terminal methionine to the produced protein.[23] Cysteine mutants were confirmed by DNA sequencing on an ABI 3700 (Applied Biosystems). Proteins were produced and purified as described previously,[35] and the concentrations were determined spectrophotometrically using the extinction coefficients $\epsilon_{280} = 5690\ M^{-1}\ cm^{-1}$ for Z_{SPA-1} and Z_{SPA-1} mutants in the reduced state, $\epsilon_{280} = 5810\ M^{-1}\ cm^{-1}$ for mutants in the oxidized state, and $\epsilon_{275} = 1400\ M^{-1}\ cm^{-1}$ for the Z domain.

Gel Electrophoresis. Purified proteins were analyzed with SDS-PAGE for which 5 μL of 175 μM samples were loaded on a Criterion 4−12% (BLS-Tris) gel in MES buffer (Bio-Rad) after heating at 70 °C for 10 min and addition of 0.3 μL of 1 M dithiothreitol (DTT) reducing agent. No other bands than those of monomeric Z_{SPA-1} mutants could be detected on the gels following Coomassie staining, with the exception of mutant 1 for which a weak band (<5%) corresponding to the dimeric form was also observed.

Mass Spectrometry. Protein samples were dialyzed against H_2O, diluted to 10 μM in 50% acetonitrile and 0.2% formic acid, and analyzed by electrospray-ionization mass spectrometry (ESI-MS) on a Q-TOF micromass spectrometer (Manchester, UK). Correct formation of disulfide bonds was verified by comparing masses recorded with and without 1mM tris(2-carboxyethyl)phosphine (TCEP; Sigma-Aldrich) reducing agent.

Circular Dichroism Spectroscopy. Circular dichroism (CD) was measured on a Jasco J-810 spectropolarimeter equipped with a Peltier type temperature controller (Jasco PTC-423S) using 25 μM protein in 20 mM potassium phosphate buffer at pH 5.6 and a 0.1-cm cuvette cell. The CD spectrum between 260 and 200 nm was recorded at 10 °C, and thermal denaturation from 10 to 95 °C was monitored at 222 nm using a heating rate of 5 °C min^{-1} and a detection response time of 1 s.

Thermal melting profiles were analyzed assuming a two-state model for protein unfolding. The observed mean residue ellipticity (MRE) is

$$[\theta]_{obsd} = (1 - f_{unfold}(T))[\theta]_N + f_{unfold}(T)[\theta]_U \quad (1)$$

where $[\theta]_N$ and $[\theta]_U$ represent temperature-dependent MRE of the native and unfolded states, respectively. The fraction of unfolded protein f_{unfold} is related to the equilibrium unfolding constant K_{unfold} as

$$f_{unfold}(T) = \frac{K_{unfold}(T)}{K_{unfold}(T) + 1} \quad (2)$$

The temperature dependence of K_{unfold} can be described using the following parametrization of the Gibb's free energy difference, ΔG°_{unfold}

$$K_{unfold}(T) = \exp\left(\frac{-\Delta G^\circ_{unfold}(T)}{RT}\right) = \exp\left(\left(\frac{-1}{RT}\right)\left(\Delta H^\circ_{unfold}(T_m)\left(1 - \frac{T}{T_m}\right) + \Delta C^\circ_{P,unfold}\left(T - T_m - T\ln\frac{T}{T_m}\right)\right)\right) \quad (3)$$

where R is the gas constant, and T_m is the (melting) temperature at which $\Delta G^\circ_{unfold}(T_m) = 0$, $\Delta H^\circ(T_m)$ is the unfolding enthalpy at T_m. If the heat capacity change $\Delta C^\circ_{P,unfold}$ either equals zero or is undeterminable in the melting experiments, then $\Delta H^\circ(T_m)$ corresponds to the van't Hoff enthalpy.

Equations 1 to 3 were fitted to experimental data using nonlinear least-squares regression routines available within Origin 7.0 (OriginLab Corporation, 2002). MRE values were assumed to be linear functions of temperature;[36] $[\theta]_N = a_N + b_N T$ and $[\theta]_U = a_U + b_U T$. The values of the four a_N, b_N, a_U, and b_U coefficients were determined by optimization together with the thermodynamics parameters. However, they were restricted so that common values of a_U, b_N, and b_U were determined for all Z_{SPA-1} mutants in the oxidized state, and common values of b_N and b_U were determined for the reduced state mutants. In addition, we tested the possibility that $\Delta C^\circ_{P,unfold}$ is insignificantly small by comparing the F-statistics[37] for fits with a fixed value $\Delta C^\circ_{P,unfold} = 0$ to fits in which $\Delta C^\circ_{P,unfold}$ was an adjustable parameter. Standard errors in best-fit values were calculated from the covariance matrix.

Isothermal Titration Calorimetry (ITC). Binding of Z_{SPA-1} mutants to the Z domain was studied using an MCS-ITC titration microcalorimeter (MicroCal Inc, Northampton, MA) with a cell volume of 1.36 mL. All solutions were degassed before the experiments, which were performed in 20 mM potassium phosphate buffer at pH 5.6 with or without 1 mM TCEP reducing agent. The protein samples were dialyzed against the same batch of buffer prior to experiments to minimize artifacts due to minor differences in buffer composition. Solutions of the Z domain at 350 to 450 μM concentrations were injected into the calorimeter cell containing 25 to 40 μM Z_{SPA-1} mutant. A typical experiment consisted of a 5 μL preliminary injection followed by 24 subsequent 10 μL injections. Reaction heats observed toward the end of the titrations were similar to the heats of dilution measured in control experiments where Z was titrated into buffer. Baseline correction and integration of the calorimeter response was carried out using the Origin software (MicroCal Inc.) provided with the calorimeter. Binding enthalpy values were corrected for heats of dilution and fitted to a model in which the variable parameters are the stoichiometry of identical sites (n), an apparent dissociation constant (K_d^{app}), and calorimetric reaction enthalpy (ΔH_{ITC}).

The calorimetrically measured ΔH_{ITC} contains contributions from the intrinsic binding event and the enthalpy of folding of any fraction f_{unfold} of Z_{SPA-1}, as shown previously.[17] A corrected binding enthalpy, ΔH°_{bind}, is obtained by subtracting the folding contribution:

$$\Delta H^\circ_{bind}(T) = \Delta H_{ITC} - f_{unfold}\Delta H^\circ_{fold}(T) = \Delta H_{ITC} + f_{unfold}(\Delta H^\circ_{unfold}(T_m) + (T - T_m)\Delta C^\circ_{P,unfold}) \quad (4)$$

where $\Delta H^\circ_{fold} = -\Delta H^\circ_{unfold}$. The f_{unfold} and ΔH°_{unfold} values were either obtained from the analysis of thermal stability described above or determined by combining MRE and ITC data to obtain folding and binding thermodynamics parameters simultaneously in a global fit of eqs 1 to 4, in analogy with a recently published procedure.[38] A corresponding correction is not needed for the more stable Z domain ($T_m = 79$ °C).

Similarly, the apparent dissociation constant measured by ITC (K_d^{app}) contains contributions from the actual binding reaction (dissociation constant K_d) as well as from folding of Z_{SPA-1}, so that

$$K_d(T) = \frac{K_d^{app}(T)}{1 + K_{unfold}(T)} \quad (5)$$

(35) Lendel, C.; Wahlberg, E.; Berglund, H.; Eklund, M.; Nygren, P.-Å.; Härd, T. *J. Biomol. NMR* **2002**, *24*, 271−272.
(36) Scholtz, J. M.; Quian, H.; York, E. J.; Stewart, J. M.; Baldwin, R. L. *Biopolymers* **1991**, *31*, 1463−1470.
(37) Devore, J. L. *Probability and statistics for engineering and the sciences*, 4th ed.; Wadsworth Inc./International Thomson Publishing Inc.: USA, 1995.
(38) Cliff, M. J.; Williams, M. A.; Brooke-Smith, J.; Barford, D.; Ladbury, J. E. *J. Mol. Biol.* **2005**, *346*, 717−732.

from which the free energy for the binding reaction ΔG°_{bind} can be obtained as

$$\Delta G^{\circ}_{bind}(T) = -RT \ln\left(\frac{1}{K_d(T)}\right) = -RT \ln\left(\frac{1 + K_{unfold}(T)}{K_d^{app}(T)}\right) \quad (6)$$

The binding entropy was then determined as $-T\Delta S^{\circ}_{bind}(T) = \Delta G^{\circ}_{bind}(T) - \Delta H^{\circ}_{bind}(T)$. We note that all thermodynamic quantities reported here are calculated based on macromolecular concentrations and neglecting any nonideality of the solutions. They are therefore only relevant at specific buffer and concentration conditions.

NMR Spectroscopy. NMR samples contained 0.2 to 0.9 mM ^{15}N-labeled protein in 20 mM potassium phosphate buffer, pH 5.6 with 10% (v/v) D_2O. Reduced samples contained 5 to 10 mM TCEP. ^{15}N-HSQC experiments were performed at 20 °C on a Bruker Avance 600 MHz spectrometer with 128 t_1 increments using echo/antiecho-TPPI for phase sensitivity in the indirect dimension and with 4 to 128 recorded transients per increment.

Results

Formation and Verification of Disulfides in Z_{SPA-1}. Six double cysteine Z_{SPA-1} mutants were designed, and five of these were successfully produced and purified. Affinity chromatography with protein A linked to a resin was used as a first purification step so that binding affinity for the Z domain was a determinant already during protein purification. Mutant 6:A12C/S41C could not be purified in amounts detectable by SDS-PAGE, and the reason can therefore be that it does not bind to protein A. Monomeric fractions of the other five mutants were purified by size exclusion chromatography (SEC) under (air) oxidizing conditions. Oxidized dimers and multimers were also present before SEC, but the monomeric form was dominating, except for samples of 1:D2C/S39C in which about two-thirds of the protein is in dimeric or multimeric forms. The SEC retention volumes of monomeric mutants are concentration dependent, and the proteins migrate slower than expected based on their molecular weight (not shown). The elution peaks also show characteristic tailing. The tendency for self-association of Z_{SPA-1} at high concentrations[15,16] is therefore present also in the cystein mutants.

Protein identities and the presence of oxidized disulfides were confirmed by mass spectrometry (see Supporting Information). The difference in mass corresponding to two hydrogens lost upon disulfide bond formation could be measured precisely. All protein samples contain 20 to 40% of a species with a molecular weight of +131 Da corresponding to an unprocessed N-terminal methionine residue. Samples of mutants 2 and 4 in the oxidized state also contain a small fraction of a species that is 32 Da heavier than expected. This modification is not detectable in the presence of TCEP reducing agent. The +32 mass difference is not consistent with oxidation of one or both of the cysteine thiols to sulfinic or sulfenic acid,[39] respectively, because such modifications would result in differences of +34 (one −SOOH and one −SH, or two −SOH) compared to the disulfide-containing species (−S−S−). The additional oxidation might be hydroxylation of a proline residue, but this cannot be concluded based on the present data. In any case, the modification appears to be harmless in terms of structure and Z domain binding properties, because oxidized mutant 2 and 4 samples do not show any anomalies compared to the other mutants in thermal melting or binding experiments.

(39) Kim, J. S.; Raines, R. T. *Eur. J. Biochem.* **1994**, *224*, 109−114.

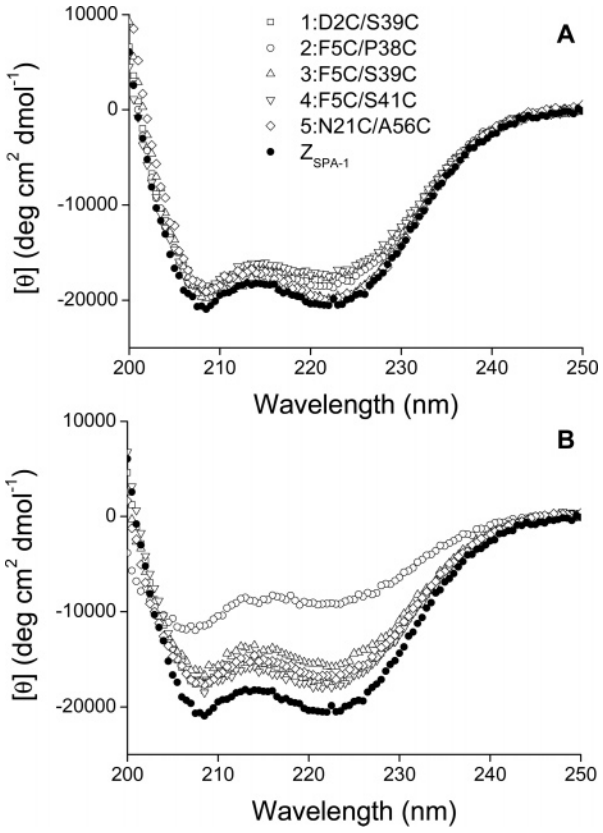

Figure 2. Circular dichroism (MRE) of Z_{SPA-1} and five Z_{SPA-1} cystein mutants as indicated (A) under air oxidizing conditions and (B) in the presence of 1 mM TCEP reducing agent (the same data set is shown for Z_{SPA-1} in the two panels).

Table 1. Thermal Stability Z_{SPA-1} and Five Double Cystein Z_{SPA-1} Mutants[a]

protein	T_m (°C)	$\Delta H^{\circ}_{unfold}(T_m)$[b] (kcal mol^{-1})	$[\theta]_N$ (20 °C)[c] (deg cm^2 dmol^{-1} × 10^3)
0: Z_{SPA-1}	40.3 ± 0.2	30.0 ± 0.6	−19.9 ± 0.1
1: D2C/S39C			
(ox)[d]	45.6 ± 0.2	24.6 ± 0.4	−19.2 ± 0.1
(red)[e]	37.5 ± 0.3	27.6 ± 0.8	−16.3 ± 0.1
2: F5C/P38C			
(ox)	41.6 ± 0.2	24.7 ± 0.5	−18.4 ± 0.1
(red)	(<20)	n.d.[f]	n.d.
3: F5C/S39C			
(ox)	52.6 ± 0.2	30.3 ± 0.5	−19.3 ± 0.1
(red)	23 ± 4	n.d.	n.d.
4: F5C/S41C			
(ox)	55.9 ± 0.2	31.7 ± 0.6	−17.0 ± 0.1
(red)	45.6 ± 0.3	32.9 ± 1.0	−16.6 ± 0.1
5: N21C/A56C			
(ox)	71.5 ± 0.2	31.8 ± 0.5	−19.6 ± 0.1
(red)	26 ± 3	n.d.	n.d.

[a] From fits of thermal denaturation data in Figure 3 to eqs 1 to 3. [b] van't Hoff enthalpy for $\Delta C^{\circ}_{P,unfold} = 0$. [c] Mean residue ellipticity (MRE) at 222 nm for native (folded) protein; best-fit value of $[\theta]_N$ in eq 1 at 20 °C. [d] As purified under air oxidation. [e] After addition of 1 mM TCEP reducing agent. [f] Not determined.

Folding and Stability. The α-helical content of the Z_{SPA-1} mutants was analyzed by circular dichroism (Figure 2 and Table 1), and the stability was monitored in thermal unfolding experiments (Figure 3). All CD spectra show negative minima at 208 and 222 nm, and the signal changes sign from negative

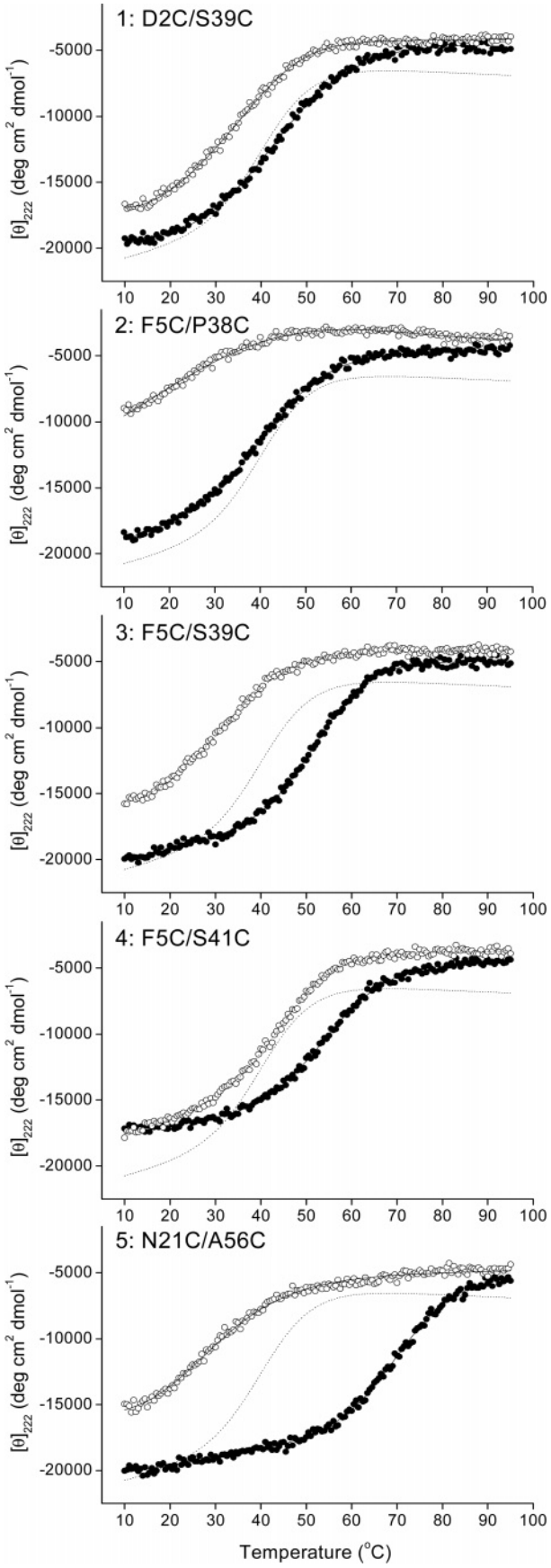

Figure 3. Thermal denaturation of Z_{SPA-1} (dashed line) and Z_{SPA-1} mutants under air oxidizing conditions (●) and after addition of 1 mM TCEP reducing agent (○) monitored as MRE at 222 nm. The solid lines indicate fits to eqs 1 to 3. Best-fit parameters are shown in Table 1.

to positive at 202 nm. These are characteristic features of a predominantly helical secondary structure. The helical content of oxidized mutants is in all cases equal to or marginally (<15%) lower than that of wild-type Z_{SPA-1}. Under reducing conditions all five mutants have a lower α-helical content than Z_{SPA-1}. For mutants 2, 3, and 5 this is partly caused by significant thermal unfolding already at 10 °C (Figure 3). The disulfide cross-link does not appear to have any effect on the secondary structure content in mutant 4:F5C/S41C.

The melting curves in Figure 3 were fit to eqs 1 to 3 to quantify the unfolding equilibrium. Parameters relating to the MRE of the unfolded states and the temperature dependence of the MRE were locked to common values in global fits. Values of the melting temperature T_m and the unfolding enthalpy at the transition midpoint ($\Delta H^\circ_{unfold}(T_m)$) could be determined in most cases, but statistically significant values of the unfolding heat capacity $\Delta C^\circ_{P,unfold}$ could not be resolved. Best-fit values of T_m and the (van't Hoff) ΔH°_{unfold} obtained when the heat capacity term in eq 3 is omitted from the fit are shown in Table 1 together with the native state MRE values ($[\theta]_N$ at 20 °C). Results from a full fit of all parameters in eq 3 can be found as Supporting Information.

Thermal stabilities of the mutants in the oxidized state are in all cases higher than that of wild-type Z_{SPA-1} for which T_m = 40 °C, but none of the mutants compare to the high T_m (79 °C) value of the original Z-domain.[15,17] The largest effect is observed in mutant 5:N21C/A56C where the disulfide restraining the C-terminus to the loop between helices I and II results in a T_m > 70 °C. Disulfides linking the N-terminus to the loop between helices II and III have smaller effects, although the T_m increase compared to Z_{SPA-1} is significant in mutants 3 (T_m = 53 °C) and 4 (T_m = 56 °C). Under reducing conditions the thermal stability was lowered by 4 °C to 13 °C compared to Z_{SPA-1}, except for mutant 4:F5C/S41C in which the cysteines actually improve thermal stability also in the reduced state. The largest T_m difference between oxidized and reduced states is observed with mutant 5 (ΔT_m > 40 °C). Mutant 2:F5C/P38C is the least stable of the five mutants in both oxidized and reduced states and only marginally more stable than Z_{SPA-1} in the oxidized state. Apparently, the substitution of Pro38 in the second loop to cysteine is critically destabilizing.

The ^{15}N HSQC NMR spectrum of Z_{SPA-1} shows the characteristics of a protein in which interconversion between multiple poorly packed and/or unfolded conformations leads to averaging and differential line broadening.[15,16] We recorded the ^{15}N-HSQC spectrum of the five Z_{SPA-1} mutants under oxidizing and reducing conditions to monitor overall differences in conformational homogeneity and backbone hydrogen bond stability. The NMR spectrum of mutants 3:F5C/S39C and 4:F5C/S41C is compared to those of Z_{SPA-1} and the Z domain in Figure 4. Disulfide formation improves the appearance of the NMR spectrum of 3:F5C/S39C and 5:N21C/A56C, for which more and sharper cross-peaks compared to Z_{SPA-1} suggest a stabilization of the MG-state conformation. Reducing conditions in general lead to poor resonance dispersion and severe line broadening, suggesting poorer packing and/or a shift in the equilibrium in favor of more unfolded states. Mutant 4:F5C/S41C is an exception where the disulfide bridge appears to induce conformational heterogeneity (Figure 4). The effect cannot be due to the alternative covalent modification detected

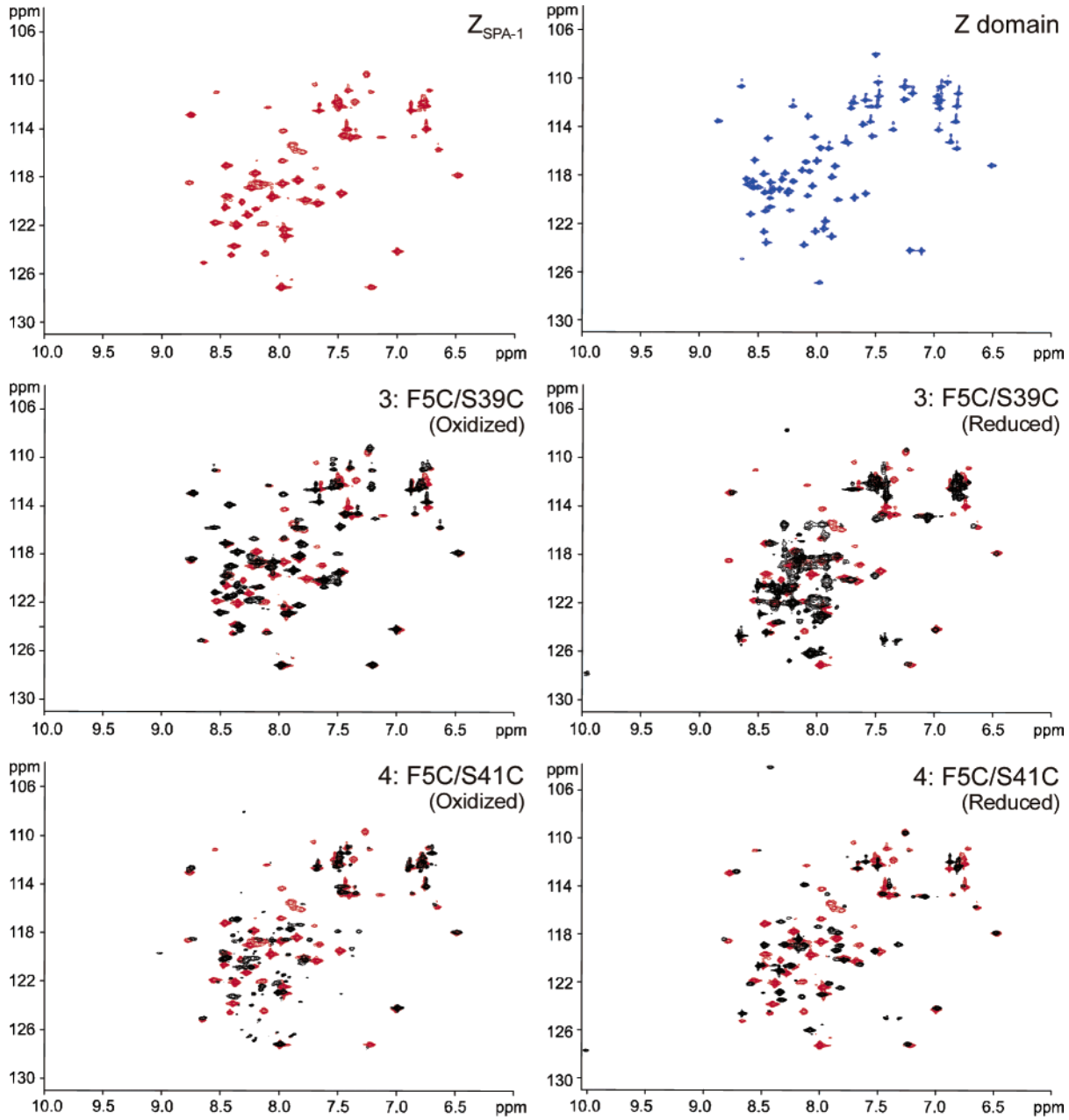

Figure 4. ^{15}N-HSQC spectrum of Z_{SPA-1}, the original Z domain, and two Z_{SPA-1} cysteine mutants in oxidized and reduced states, as indicated. Mutant spectra have been overlaid on the Z_{SPA-1} spectrum (in red) for comparison. Protein concentrations are 0.9 mM Z_{SPA-1}, 2.7 mM Z domain, 0.9 mM mutant 3, and 0.8 mM mutant 4.

by MS, because this modification is only present in a minor fraction of the sample.

Z-Domain Binding Thermodynamics. The binding of Z_{SPA-1} and five Z_{SPA-1} double cysteine mutants to the Z domain was measured by isothermal titration calorimetry (ITC; Figure 5 and Table 2). The binding affinity of disulfide-containing mutants at 21 °C ranges from being more than 10 times stronger than that of Z_{SPA-1} (mutant 3) to moderately stronger or comparable (mutants 1, 2, and 5) to significantly weakened (mutant 4). There is no correlation between thermal stability and binding affinity, except for that the strongest binder (3:F5C/S39C) is more stable than Z_{SPA-1} and has the same helical content. The binding affinity of mutant 5:N21C/A56C with the highest T_m value of all mutants is only slightly improved. The effect of disulfides is in most cases removed when these are reduced with 1 mM TCEP, as expected. The weaker binding of reduced mutant 2 can be explained by the poor thermal stability. One of the mutants (4: F5C/S41C) binds stronger in the reduced state than in the oxidized state. We attribute the small value of the stoichiometry $n = 0.85 \pm 0.07$ in Table 2 to uncertainties in protein concentration measurements.

The enthalpies measured by ITC (ΔH_{ITC}) were corrected for contributions from folding to obtain values that reflect only the binding process (ΔH°_{bind}), as described above (Table 2). The corrections for binding under oxidizing conditions at 21 °C are small (less than 1.5 kcal mol^{-1}). Corrections could not be made for mutants 2, 3, and 5 at reducing conditions, because poor thermal stabilities prohibit an accurate calculation of f_{unfold} at room temperature. Apparent binding affinities (K_d^{app}) were also

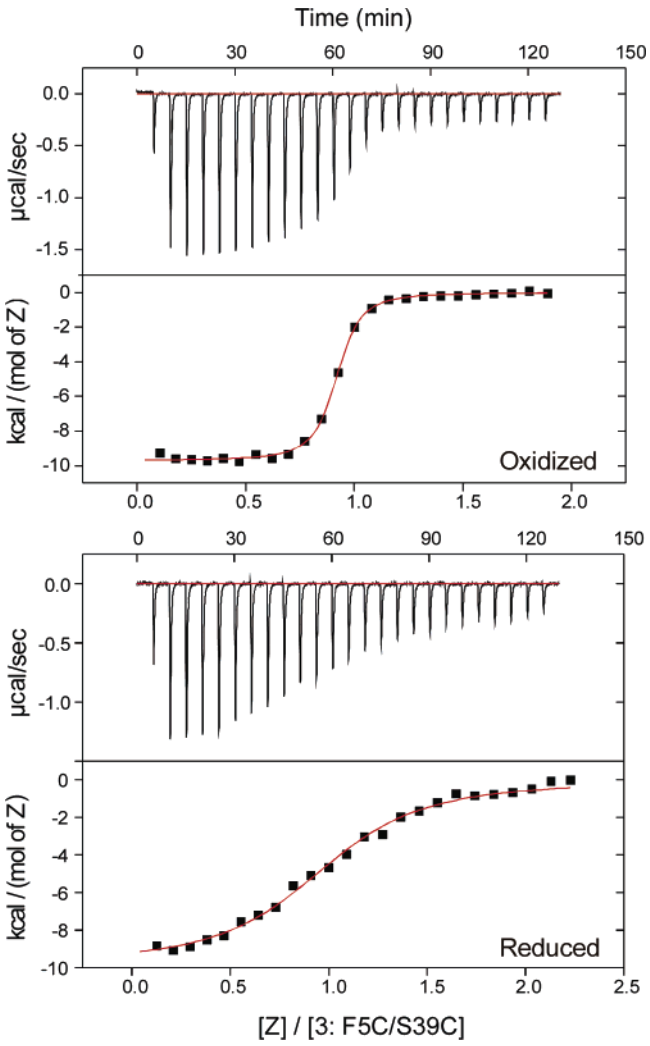

Figure 5. Isothermal titration calorimetry of oxidized or reduced Z_{SPA-1} mutant 3:F5C/S39 binding to the Z domain, as indicated. Each panel contains the calorimeter power response (top) and integrated heats (bottom), and red lines represent the corrected baselines and the best-fit binding isotherms, respectively. Binding parameters are shown in Table 2.

corrected to obtain microscopic dissociation constants (K_d), but these corrections are negligible (Table 2). There is a strong correlation between the binding enthalpy and affinity. For instance, the stronger binding by mutants 3 and 2 is more enthalpically favored ($\Delta H^\circ_{bind} = -9.6$ and -7.4 kcal mol^{-1}, respectively) than that for wild-type Z_{SPA-1} ($\Delta H^\circ_{bind} = -4.5$ kcal mol^{-1}), whereas the poorest binder (oxidized mutant 4) shows less favorable binding enthalpy (-2.5 kcal mol^{-1}). Furthermore, binding is more enthalpically favorable in the reduced than in the oxidized state in the two cases (mutants 1 and 4) where corrected values for the reduced states could be obtained. However, this trend does not hold for mutant 3 where a corrected binding enthalpy for the reduced state would be smaller (less negative) than that in the oxidized state at 21 °C.

Additional experiments in the temperature range 10 to 30 °C were performed on the strongest binder (mutant 3:F5C/S39C) to characterize its binding thermodynamics in more detail (Table 2). The uncorrected binding enthalpy of wild-type Z_{SPA-1} is a nonlinear function of temperature, and we previously showed that the nonlinearity is due to a temperature-dependent shift of the unfolding equilibrium of Z_{SPA-1} upon binding to Z.[17] A similar scenario exists for mutant 3, but the nonlinearity is less pronounced as expected for a more stable protein. In both cases, corrections for folding lead to linear temperature dependencies (Figure 6). The binding heat capacity for mutant 3 obtained in this way is $\Delta C^\circ_{P\,bind} = -190 \pm 30$ cal mol^{-1} K^{-1}. Similar values are obtained from the slope of uncorrected ΔH_{ITC} vs temperature at low temperatures (when the fraction unfolded is insignificant) or in a simultaneous fit of folding and binding data (see Supporting Information). This heat capacity change is significantly smaller than that of wild-type Z_{SPA-1} ($\Delta C^\circ_{P,bind} = -400 \pm 30$ cal mol^{-1} K^{-1}), and the difference reflects a fundamental distinction in binding thermodynamics to be discussed below. All binding thermodynamics data have been summarized in Table 3.

Discussion

Z_{SPA-1} binds to the Z domain with a dissociation constant $K_d = 0.5$ to 2 μM, depending on temperature, buffer, and pH.[17] A comparison of the binding interface in Z:Z_{SPA-1} with that of the naturally occurring complex between the B domain of protein A and an IgG Fc domain reveals a number of common features, and Z_{SPA-1} and Fc induce similar rearrangements of side chains on the Z (or B) domain surface.[15,40] (The B and Z domains share 97% sequence identity, and the surfaces of helices I and II are identical.) We previously investigated different reasons to why the Z:Z_{SPA-1} complex is not formed with an affinity in the 20 to 70 nM range as the case for Z:Fc. Several lines of evidence suggested that the need for conformational stabilization of Z_{SPA-1} in the complex is energetically costly and more serious for optimal affinity than the poor thermal stability of the free state or the composition of the binding surface.[17] We decided to investigate this possibility further by introducing disulfide bridges to stabilize the unbound affibody. We find that binding can be improved more than 10-fold; mutant 3 binds with $K_d = 130 \pm 20$ nM at room temperature. This result shows that the phage-display selected binding surface is close to optimal and that conformational stabilization of the free affibody component can bring Z binding affinity into a range that is close to that evolved by Nature. Below we discuss the structural and thermodynamic basis for this improvement.

Structure and Stability of the Mutants and the Relation to Binding Affinity. The five disulfide mutants that could be produced are all more stable than wild-type Z_{SPA-1} in their oxidized states. The conformational properties have in some cases also been improved as evidenced by a larger number of sharp amide resonances in the NMR spectrum indicating better backbone hydrogen bonding and less conformational flexibility (for instance in the spectrum of mutant 3 in Figure 4). However, both NMR and CD data show that the structures of disulfide-containing mutants still are less ordered than that of the Z domain. For instance, even in the best-binding mutant 3 it is not possible to completely assign the backbone NMR resonances of helices I and II, due to broadened amide resonances and missing medium-range NOE connectivities (not shown). The remaining transient unfolding of these helices is also manifested in the average helix content. None of the mutants has a larger helix content than wild-type Z_{SPA-1} in which the average helicity in the free state still is only ca. 75% of that in the bound state.[16,17]

(40) Deisenhofer, J. *Biochemistry* **1981**, *20*, 2361−2370.

Table 2. ITC Data for Binding of Z_{SPA-1} and Five Z_{SPA-1} Mutants to the Z Domain

	values from ITC				corrected for folding[a]		
protein	temp (°C)	ΔH_{ITC} (kcal mol^{-1})	K_d^{app} (μM)	n	f_{unfold}	ΔH°_{bind} (kcal mol^{-1})	K_d (μM)
0: Z_{SPA-1}	21.2	−5.7 ± 0.1	1.6 ± 0.1	0.81 ± 0.01	0.039	−4.5 ± 0.1	1.5 ± 0.1
1: D2C/S39C							
(ox)[b]	21.3	−5.6 ± 0.5	0.8 ± 0.05	0.75 ± 0.01	0.039	−4.6 ± 0.8	0.8 ± 0.05
(red)[c]	21.2	−8.6 ± 0.5	1.2 ± 0.1	0.86 ± 0.01	0.078	−6.4 ± 1.5	1.1 ± 0.1
2: F5C/P38C							
(ox)	20.6	−8.8 ± 0.5	0.5 ± 0.05	0.80 ± 0.01	0.056	−7.4 ± 1.0	0.5 ± 0.05
(red)	20.9	−1.4 ± 0.5	3.2 ± 0.3	0.77 ± 0.01	n.d.[d]	n.d.	n.d.
3: F5C/S39C							
(ox)	11.5	−8.0 ± 0.5	0.15 ± 0.02	0.87 ± 0.01	0.001	−8.0 ± 0.5	0.15 ± 0.02
	15.7	−9.5 ± 0.5	0.22 ± 0.02	0.88 ± 0.01	0.003	−9.4 ± 0.5	0.22 ± 0.02
	21.1	−9.8 ± 0.5	0.13 ± 0.02	0.89 ± 0.01	0.007	−9.6 ± 0.5	0.13 ± 0.02
	25.3	−11.2 ± 0.5	0.19 ± 0.02	0.90 ± 0.01	0.014	−10.8 ± 0.6	0.19 ± 0.02
	30.1	−12.6 ± 0.5	0.19 ± 0.02	0.89 ± 0.01	0.030	−11.7 ± 0.8	0.19 ± 0.02
(red)	20.6	−9.8 ± 0.5	2.0 ± 0.2	0.99 ± 0.01	n.d.	n.d.	n.d.
4: F5C/S41C							
(ox)	21.4	−2.6 ± 0.5	3.1 ± 0.3	0.74 ± 0.01	0.003	−2.5 ± 0.5	3.1 ± 0.3
(red)	20.8	−5.5 ± 0.5	1.2 ± 0.1	0.81 ± 0.01	0.014	−5.0 ± 0.6	1.2 ± 0.1
5: N21C/A56C							
(ox)	21.4	−5.0 ± 0.5	1.1 ± 0.1	0.79 ± 0.01	0.000	−5.0 ± 0.5	1.1 ± 0.1
(red)	21.0	−5.7 ± 0.5	1.1 ± 0.1	0.94 ± 0.01	n.d.	n.d.	n.d.

[a] Binding parameters corrected for the shift in equilibrium between native and completely unfolded states of Z_{SPA-1} and mutants. [b] As purified under air oxidation. [c] After addition of 1 mM TCEP reducing agent. [d] Not determined.

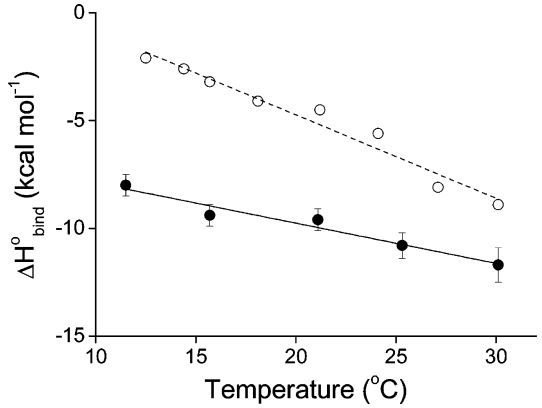

Figure 6. Corrected binding enthalpies for Z_{SPA-1} (○; data from ref 17) and the oxidized form of mutant 3:F5C/S39C (●) as a function of temperature. The lines indicate linear fits to determine $\Delta C^\circ_{P,bind} = -400 \pm 30$ cal mol^{-1} K^{-1} for Z_{SPA-1} (dashed) and $\Delta C^\circ_{P,bind} = -190 \pm 30$ cal mol^{-1} K^{-1} for 3:F5C/S39C (solid).

The amino acids selected for substitution with cysteines were mainly chosen to covalently stabilize helices I and II since these constitute the binding surface. In one case (5:N21C/A56C) the disulfide connects helix II to helix III, and this is in fact the most stable mutant. Stabilization of the interaction between helices I and II does not have the same influence on thermal stability even though a significant increase in T_m is observed in two mutants. On the other hand, we find that the thermal stability differences observed here are not critical for high-affinity binding. This is illustrated by the absence of a correlation between melting temperatures and dissociation constants for the complexes (Tables 2 and 3). It is also supported by a comparison of the Z-binding affinity of wild-type Z_{SPA-1} ($K_d = 1.6$ μM) with that of the cysteine mutants in the reduced state: apparent K_d values of the latter fall within the range 1.1 to 3.2 μM, and mutants 1 and 5 bind stronger than the wild-type even though their (reduced state) T_m values are significantly lower. The relatively small effect of shifts in the folded−unfolded state equilibrium on binding affinity is also apparent from eq 5. As pointed out earlier,[17] a shift from a situation in which the affibody is completely folded to one in which 50% of the unfolded state is populated ($K_{unfold} \approx 0$ and $K_{unfold} = 1$, respectively) reduces the effective binding affinity by a factor of 2 only. This is in fact also the case with mutant 2 in the reduced state: the T_m value is lower than 20 °C, and the MRE value suggests that the folded conformation is less than 50% populated at room temperature, but the binding affinity for the Z domain is not reduced by more than a factor of 2 compared to wild-type Z_{SPA-1}. Hence, it is clear that the conformational consequences of disulfide formation are more important than improving the folding−unfolding stability. This is particularly evident with mutant 4:F5C/S41C, which binds stronger in the reduced than in the oxidized state. The disulfide in this mutant apparently introduces a conformational strain which prohibits the formation of the correct binding surface. An alternative explanation to why thermal stability is unrelated to binding affinity is that an increased population of the folded state occurs due to a "destabilization" of the unfolded state without change in conformational properties of the folded state. This may be the case with mutant 5, which has been stabilized considerably with only a marginal effect on binding affinity.

Folding Thermodynamics. The effect of disulfide bonds on protein folding thermodynamics is a matter of discussion. Improved stability is likely to have a significant entropic component, because covalent linkage of distant parts of the sequence can be expected to decrease the conformational entropy of the unfolded state.[7−9] Stability improvement achieved in this way can be considered to result from destabilization of the unfolded state, as discussed above. Yet, enthalpic contributions have also been observed.[10−12] A purely entropic effect would manifest itself as an unchanged or smaller unfolding enthalpy of the more stable oxidized (disulfide-containing) protein compared to the reduced protein. (A comparison of a disulfide-containing mutant to the wild-type is not meaningful.) The thermal stability of three of the Z_{SPA-1} mutants in the reduced state is too poor to allow for a quantification of unfolding thermodynamics, and the disulfide effect can therefore only be

Table 3. Thermodynamics for Binding of Z_{SPA-1} and Five Z_{SPA-1} Mutants to the Z Domain[a]

	binding thermodynamics					entropy balance (cal mol^{-1} K^{-1})			
protein	$\Delta C^\circ_{P,bind}$ cal mol^{-1} K^{-1}	ΔH°_{bind} kcalmol^{-1}	$-T\Delta S^\circ_{bind}$ kcal mol^{-1}	ΔG°_{bind} kcal mol^{-1}	K_d (μM)	ΔS°_{bind}	ΔS°_{solv}[b]	ΔS°_{conf}[c,d]	ΔS°_{rt}[d]
0: Z_{SPA-1}[e]	-400 ± 30	-4.5 ± 0.1	-3.3 ± 0.4	-7.8 ± 0.3	1.5 ± 0.1	11 ± 2	109 ± 7	-90 ± 9 (-74 ± 9)	-8 (-24)
1: D2C/S39C									
(ox)[f]	n.d.[h]	-4.6 ± 0.8	-3.6 ± 1.2	-8.2 ± 0.4	0.8 ± 0.05	12 ± 4			
(red)[g]	n.d.	-6.4 ± 1.5	-2.5 ± 1.9	-8.0 ± 0.4	1.1 ± 0.1	8 ± 6			
2: F5C/P38C (ox)	n.d.	-7.4 ± 1.0	-1.0 ± 1.4	-8.4 ± 0.4	0.5 ± 0.05	4 ± 5			
3: F5C/S39C (ox)	-190 ± 30	-9.6 ± 0.5	0.4 ± 0.9	-9.2 ± 0.4	0.13 ± 0.02	-1 ± 3	52 ± 7	-45 ± 10 (-29 ± 10)	-8 (-24)
4: F5CS41C									
(ox)	n.d.	-2.5 ± 0.5	-4.9 ± 0.9	-7.4 ± 0.4	3.1 ± 0.3	17 ± 3			
(red)	n.d.	-5.0 ± 0.6	-2.9 ± 1.0	-7.9 ± 0.4	1.2 ± 0.1	10 ± 4			
5: N21C/A56C (ox)	n.d.	-5.0 ± 0.5	-3.0 ± 0.9	-8.0 ± 0.4	1.1 ± 0.1	10 ± 4			

[a] At 21 °C. [b] Calculated as $\Delta C^\circ_{P,bind} \times \ln(T/385)$. [c] From eq 8. [d] Alternative values represent uncertainties in ΔS°_{rt}, as discussed in the text. [e] Data from ref 17. [f] Oxidized state. [g] Reduced state. [h] Not determined.

monitored for mutants 1 and 4. In these cases the data seem to suggest that the entropic contributions might be dominating, because the van't Hoff enthalpies for unfolding are smaller in the oxidized states than in the reduced states (Table 1). However, the uncertainties associated with the $\Delta C^\circ_{P,unfold}$ values prohibit a firm conclusion. Complementary differential scanning calorimetry (DSC) experiments could in principle provide additional information, but mutants 1 and 4 are both unfortunately unsuitable for DSC due to self-association.

Binding Affinity and Enthalpy−Entropy Compensation. Some insight into the thermodynamic basis for improved Z-domain binding affinity can be gained from correlations between data in Table 3. First, we note a correlation between binding enthalpy and binding affinity (Figure 7A) of the disulfide-containing mutants. The correlation also includes wild-type Z_{SPA-1} and the two reduced-state mutants for which corrected ΔH°_{bind} values could be obtained. Second, there is a corresponding strong binding enthalpy−entropy compensation effect[41] in this set of eight Z_{SPA-1} variants. The plot of binding enthalpy vs binding entropy in Figure 7B has a slope of 380 K. Hence, in practical terms, every kcal mol^{-1} of binding free energy gained by one protein in the set compared to any of the others consists of an enthalpy gain of 4.4 kcal mol^{-1} and a compensating entropy loss of -3.4 kcal mol^{-1}. Increased binding affinity is therefore favored by enthalpic rather than entropic effects (which are discussed in the next section).

We suggest that the correlations are a manifestation of similar (or identical) binding interfaces in the different Z-domain complexes and different properties of the proteins in the free states. The enthalpy−entropy compensation reflects the balance between the favorable binding enthalpy of a fully binding competent conformation and the entropic cost of maintaining such a conformation in the bound state. Or in other words: there is an optimal interface in which electrostatic and surface complementarities as well as hydrogen bonding possibilities are fully explored. This conformation is the most favorable for binding from an enthalpic point of view. However, many other states are also possible. These may be less favorable enthalpically because not all contacts are formed, but they are favored for statistical reasons and therefore represent advantageous entropy in the bound state. The optimal binding interfaces of wild-type Z_{SPA-1} and the mutants in reduced and oxidized states

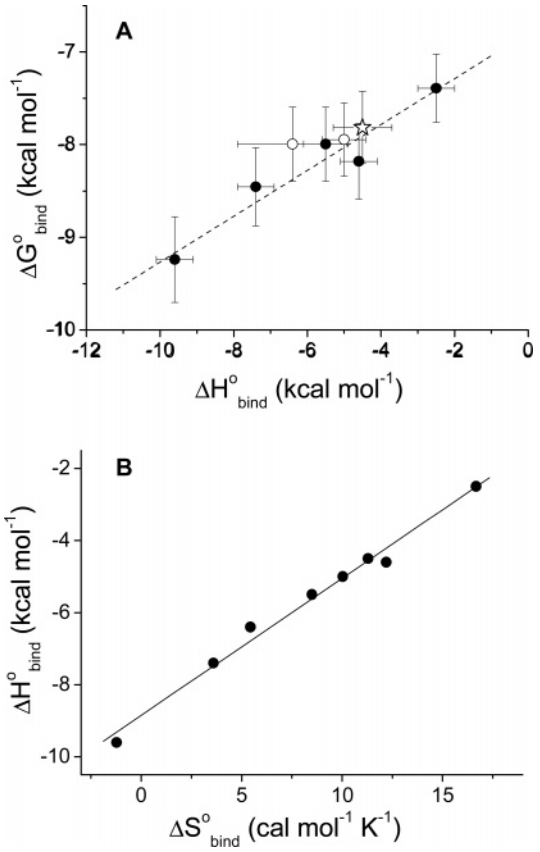

Figure 7. Correlations between thermodynamics parameters for binding of the Z_{SPA-1} affibody and five double cysteine Z_{SPA-1} mutants to the Z domain. (A) Correlation between ΔG°_{bind} and ΔH°_{bind}. Symbols represent Z_{SPA-1} (☆), oxidized Z_{SPA-1} mutants (●), and mutants 1 and 4 under reducing conditions (○). (B) Enthalpy−entropy compensation plot of ΔH°_{bind} vs ΔS°_{bind}. The slope of the solid line obtained by linear regression is 380 ± 18 K. All data can be found in Table 3.

are likely to be very similar, because residues involved in Z-binding are unaltered. However, the proteins in the set are not identical with respect to the possibilities to support the optimal contact surface. Some binders (e.g., oxidized mutant 4) form complexes with suboptimal binding interfaces (less favorable binding enthalpy) in which instead the binding entropy is more favorable due to a larger number of possible binding modes. Hence, there is a continuous scale of enthalpy−entropy compensation for binding of the different mutants.

(41) Dunitz, J. D. *Chemistry & Biology* **1995**, *2*, 709−712.

The correlation between binding affinity and binding enthalpy follows from the same arguments. The strongest binder (oxidized mutant 3) is the binder in which the optimal surface is most easily achieved. Hence there is a larger fraction of such interfaces in an ensemble of complexes, and the net enthalpy change for forming this ensemble is larger. Thus, the disulfide bonds mainly confer a larger population of binding competent species, and the most important factor for increasing the affinity is to get everything steady and neat in the right position for binding. The consequence is that the best binders pay an entropic price for the well-defined interaction surface. This line of argumentation is similar to the concepts of positively cooperative noncovalent interactions, consequent reduction in dynamics, and enthalpic stabilization of biomolecular complexes expressed in a recent review by Williams et al.[42]

A formal view of the disulfide effect on Z_{SPA-1} binding affinity can be obtained by partitioning the binding free energy into two contributions: the conformational stabilization of a binding competent species ($\Delta G^\circ_{conf.stab.}$) and the interaction of this species with the Z-domain ($\Delta G^\circ_{interaction}$) so that

$$\Delta G^\circ_{bind} = \Delta G^\circ_{conf.stab.} + \Delta G^\circ_{interaction} \quad (7)$$

With this view it is clearer that if the binding interface is unaltered in the mutants, $\Delta G^\circ_{interaction}$ must be a constant, whereas $\Delta G^\circ_{conf.stab.}$ is being changed by mutation.

Contributions to Binding Entropy. In our previous analysis of Z_{SPA-1} binding thermodynamics we proposed that conformational stabilization of MG state Z_{SPA-1} is entropically unfavorable. However, in the present data set when we compare disulfide-linked mutants to wild-type Z_{SPA-1} binding we find no large differences in the binding entropy terms. In fact, high binding affinity is correlated to favorable enthalpy rather than to entropy changes. Hence, we need to account for the effect of conformational entropy. The explanation is to be found in observed heat capacity changes and counteracting effects of desolvation and conformational contributions. Since protonation effects are negligible,[17] we may decompose the observed binding entropy into three dominating terms as[43−45]

$$\Delta S^\circ_{bind}(T) = \Delta S^\circ_{solv}(T) + \Delta S^\circ_{conf} + \Delta S^\circ_{rt} = \Delta C^\circ_{P,bind} \ln\left(\frac{T}{385}\right) + \Delta S^\circ_{conf} + \Delta S^\circ_{rt} \quad (8)$$

where ΔS°_{conf} represents changes in conformational entropy and the desolvation term $\Delta S^\circ_{solv}(T)$ is based on the assumption that entropies of desolvation of polar and nonpolar surfaces are zero at 385 K (ref 46 and work cited therein) in which case it is proportional to $\Delta C^\circ_{P,bind}$. The contribution from changes in rotational and translational entropy, ΔS_{rt}, is uncertain. To cover a reasonable range of possibilities we use the value $\Delta S^\circ_{rt} = -8$ cal mol^{-1} K^{-1} as a lower limit and $\Delta S^\circ_{rt} = -24$ cal mol^{-1} K^{-1} as an upper limit for the effect, as discussed in more detail elsewhere.[19] Given the experimental values of binding entropies and heat capacity changes we obtain $\Delta S^\circ_{solv} = 109 \pm 7$ cal mol^{-1} K^{-1} and $\Delta S^\circ_{conf} \sim -74 \pm 9$ to -90 ± 9 cal mol^{-1} K^{-1} for wild-type Z_{SPA-1}, whereas $\Delta S^\circ_{solv} = 52 \pm 7$ cal mol^{-1} K^{-1} and $\Delta S^\circ_{conf} \sim -29 \pm 10$ to -45 ± 10 cal mol^{-1} K^{-1} for oxidized mutant 3 at 21 °C (Table 3). While these numbers suffer somewhat from the uncertainty in ΔS°_{rt}, it is nevertheless clear that (i) binding of disulfide-containing mutant 3 to the Z domain involves a reduced conformational entropy change as compared to Z_{SPA-1} binding and (ii) this reduction is accompanied by a compensating and less favorable desolvation entropy. By introducing a constraining disulfide bond in Z_{SPA-1} we have therefore achieved the desired effect: the entropy loss from conformational stabilization is reduced. On the other hand, the free state of the mutant is not solvated to the same extent, and the possibility of obtaining a large and favorable desolvation effect on binding is therefore also reduced. The desolvation entropy effect is closely related to the observed heat capacity change,[45] which in turn is highly correlated to the changes in solvent-accessible surface area.[47−49] We observe a significant decrease in $\Delta C^\circ_{P,bind}$ for mutant 3 compared to wild-type Z_{SPA-1}. Structurally, the effect of the disulfide may therefore be visualized as a "tightening" of the ensemble of conformations of the free mutant 3 (lower conformational entropy) so that the average water-accessible nonpolar surface is less than that of Z_{SPA-1} (smaller desolvation effect on binding).

Acknowledgment. This work was supported by the Swedish Research Council (VR). We thank Dr. Vildan Dincbas-Renqvist (KTH) for assistance with ITC experiments, Dr. Hasse Karlsson (Göteborg University) for performing the mass spectrometric analysis, and Prof. Per-Åke Nygren (KTH) for valuable discussions and suggestions.

Supporting Information Available: A table with the results of the mass spectrometric analysis, a table with results of an analysis of thermal melting experiments including $\Delta C^\circ_{P,unfold} \neq 0$ as an adjustable parameter, and a figure illustrating the global fit of folding and binding parameters to MRE and ITC data for oxidized mutant 3. This material is available free of charge via the Internet at http://pubs.acs.org.

JA060933G

(42) Williams, D. H.; Stephens, E.; O'Brien, D. P.; Zhou, M. *Angew. Chem., Int. Ed.* **2004**, *43*, 6596−6616.
(43) Murphy, K. P. *Biophys. Chem.* **1994**, *51*, 311−361.
(44) Murphy, K. P.; Freire, E.; Paterson, Y. *Proteins: Struct., Funct., Genet.* **1995**, *21*, 83−90.
(45) Baldwin, R. L. *Proc. Natl. Acad. Sci. U.S.A.* **1986**, *83*, 8069−8073.
(46) Baker, B. M.; Murphy, K. P. *Methods Enzymol.* **1998**, *295*, 294−315.
(47) Spolar, R. S.; Livingstone, J. R.; Record, M. T. *Biochemistry* **1992**, *31*, 3947−3955.
(48) Makhatadze, G. I.; Privalov, P. L. *J. Mol. Biol.* **1993**, *232*, 639−659.
(49) Murphy, K. P.; Freire, E. *Adv. Protein Chem.* **1992**, *43*, 313−361.